2005 American Control Conference
June 8-10, 2005. Portland, OR, USA

Robust Feedback Control Design of an Ultra-Sensitive, High Bandwidth Tunneling Accelerometer

M. Khammash, Laura Oropeza-Ramos, Kimberly L. Turner
Department of Mechanical and Environmental Engineering
University of California at Santa Barbara
Santa Barbara, CA 93106

***Abstract*— Robust feedback control design of an ultra-sensitive, high-bandwidth, tunneling accelerometer is reported. The control design uses the H_∞ loop-shaping technique to shape the loop to achieve high disturbance rejection, noise attenuation, and robustness to parameter variations. While the design was performed on a linearized plant, nonlinear simulations of the tunneling accelerometer device demonstrate that the accelerometer can accurately sense forces over its control bandwidth even when its parameters have been perturbed away from their nominal values that were used in the control design.**

I. Introduction

High-bandwidth accelerometers are needed in many applications including seismic activity detection, inertial sensors (aerospace), and tracking devices. Micro-machined tunneling accelerometers are appealing for their high sensitivity [1], [3], [4], [5], however, noise [10] and reliability have been two issues hindering their long-term stability and use. Reliability is being addressed through advances in MEMS fabrication. By utilizing Single Crystal Silicon processes and careful packaging techniques reliability can be improved [2]. A key component of reliability is device robustness. Accelerometer parameters, particularly those associated with the tunneling component, are invariably uncertain and drift during the operation of the device. Designing for robustness is therefore essential for achieving both reliability and noise attenuation.

In this paper, we have designed a robust controller for a silicon micromachined tunneling accelerometer using H_∞ loop-shaping methods [11], [12]. Previous control strategies proposed for microscale tunneling accelerometers [2], [3], [6] have either used PID control and did not incorporate uncertainty in the design process, or have used the μ synthesis resulting in controllers of very high order. We show that the robust H_∞ loop-shaping offers an attractive alternative design approach for this application that offers relative simplicity, connection with classical control design methods, and relatively low order controllers. We demonstrate, in simulation, that the design is very effective over a large bandwidth while being robust to parameter variations. Experimental implementation of this controller onto a MEMS accelerometer is underway, and we hope to present experimental results in the final publication.

In accordance with the theory of quantum mechanics, electron tunneling can be experimentally observed when the gap between a pair of clean electrodes with a voltage bias V_b is sufficiently small. The resulting tunneling current is extremely sensitive to the gap separation distance. Indeed the tunneling current varies exponentially according to his gap. This fact is exploited by affixing an electrode to a suspended proof-mass that can move towards a second fixed electrode (the tunneling tip). See Figure 1. As the distance between the two electrodes changes, so does the tunneling current. Thus, the tunneling current can be used as a very sensitive measure of the displacement of the proof mass, close to the tunneling distance, which for this application is typically of the order of a nanometer (10 Å). By applying a voltage controlled electrostatic force, the position of the proof mass may be actuated. Using the tunneling current as a feedback signal, the position of the proof mass may be controlled to remain at a fixed distance from the tunneling tip. This distance must be maintained through the feedback control system despite the presence of external forces that tend to move it away from the equilibrium position. If good external force rejection is achieved, the control signal itself may be used as an accurate measure of such forces. In the case of the tunneling accelerometer, this would be captured by the voltage feedback signal supplied to the electrostatic actuator.

II. Accelerometer Model

In this section, we describe the mathematical model of the tunneling accelerometer. At rest, the proof mass is 1200 Nm away from the tunnel tip. We let x be the displacement of the proof mass from the rest position. Newton's law gives the motion of the proof mass:

$$m\frac{d^2x}{dt^2} + c\frac{dx}{dt} + kx = F_e + F_d$$

where $m = 5.2 \times 10^{-9}$ is the mass, c is the damping coefficient, and k is the spring constant. The forcing terms consist of the electrostatic force F_e, and the external disturbance

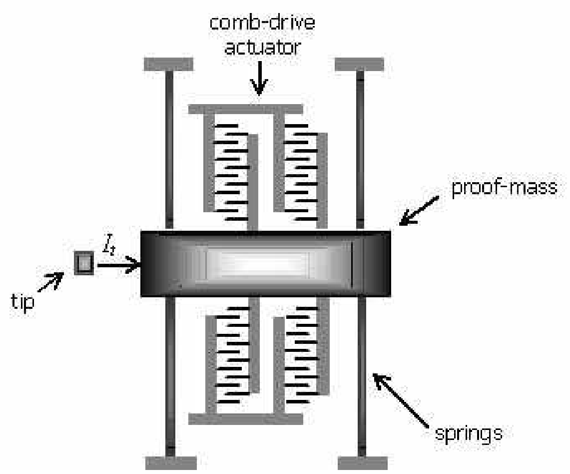

Fig. 1. Tunnelling Accelerometer

force F_d, whose measurement is the desired output of the device.

The electrostatic force exerted by the comb drive is given by

$$F_e = N\frac{\epsilon_0 h}{g}V^2,$$

where N is the number of fingers, ϵ_0 is the dielectric constant of air, h is the depth of each plate, g is the gap between the parallel electric plates, and V is the applied b across the plates of the comb drive.

Letting $\omega_0 = \sqrt{\frac{k}{m}}$ and $Q = m\frac{\omega_0}{c}$, we have

$$\frac{d^2x}{dt^2} + \frac{\omega_0}{Q}\frac{dx}{dt} + \omega_0^2 x = \frac{1}{m}\left[F_e + F_d\right]$$

The particular design considered has a proof mass of 5.2 micrograms with a spring constant $k = 6.2$ N/m. The measured value for the natural frequency ω_0 is 5.5 kHz, and $Q = 20$. The number of fingers $N = 500$, the dielectric constant of air is $\epsilon_0 = 8.854 \times 10^{-12}$ F/m, and the depth of each plate $h = 1.3 \times 10^{-5}$ m. The value of the gap between the parallel plates g has been designed so that when the tip-proof mass rest gap is $d = 1.2\ \mu m$ the actuator can close this gap with a bias voltage of 15V. Using a nominal stiffness coefficient of $k_0 = 6$ N/m, and equating $k_0 d$ to F_e we get that the designed value of $g = 1.8\ \mu m$.

A. Scaling

With the above design parameters, the problem is in need of scaling. We begin by scaling time $t \mapsto 10^{-3}t$ so that the new time variable has units of milliseconds (the frequency variable will also be krad/s). Furthermore, we scale the displacement variable $x \mapsto 10^{-9}x$ and the new x variable has units of nanometers. Combining the two scalings together we have

$$\frac{d^2x}{dt^2} + 10^{-3}\frac{\omega_0}{Q}\frac{dx}{dt} + 10^{-6}\omega_0^2 x = \frac{10^3}{m}\left(F_e + F_d\right).$$

As stated here, the forces F_e and F_d are in Newtons. It is convenient to use units of nano-Newtons to measure these forces, which we do. With these units we have

$$\frac{d^2x}{dt^2} + 10^{-3}\frac{\omega_0}{Q}\frac{dx}{dt} + 10^{-6}\omega_0^2 x = \frac{10^{-6}}{m}\left[F_e + F_d\right],$$

where $F_e = 10^9 N\frac{\epsilon_0 h}{g}V^2 (nano - Newtons)$. In the frequency domain we have: $X(s) = G(s)(F_e(s) + F_d(s))$, where

$$G(s) = \frac{\frac{10^{-6}}{m}}{s^2 + 10^{-3}\frac{\omega_0}{Q}s + 10^{-6}{\omega_0}^2}.$$

This is expressed in block diagram form in Figure 2, where $E = 10^9 N\frac{\epsilon_0 h}{g}$.

B. Tunneling Current Measurement and Feedback

In the setup of the accelerometer device, the value of x is measured only indirectly through measuring the tunneling current i. This current is proportional to the tunneling bias across the tunneling electrode gap and depends exponentially on the tunneling gap distance x_g:

$$i \propto V_b e^{-\alpha\sqrt{\phi}x_g}$$

where α is the tunneling constant, ϕ is the effective height of the tunneling barrier. For the present design, we have

$$i = 20e^{-23.719(d-x)}$$

where $d = 1200$ nm is the distance from the proof-mass and the tunneling tip when the system is at rest. The desired setpoint distance between the proof-mass and the tunneling tip is set to be 1 nm. The proof-mass displacement to be tracked is therefore 1199 nm. At this distance the bias voltage is selected so that the tunneling current is 1 nA. The control objective is now to track a 1 nA tunnel current. The closed-loop setup of this problem is shown in figure 2. An integrator is used so that the current setpoint is tracked robustly. It should be pointed out here that due to the possibility of significant drift in the tunneling parameters the measured tunneling current may not be used to solve back for the displacement. However, tracking a specific distance is not necessary. Instead what is important is that a constant distance be maintained, even if that distance cannot be determined exactly. In essence, the tunneling current will be regulated because it can be measured, but the corresponding displacement, while regulated, has an uncertain value.

III. CONTROL DESIGN

The objective of the control is to stabilize the system about the tracked equilibrium and to reject the external disturbance F_d despite uncertainty in the tunneling current/displacement relation. The system is linearized about the tracked equilibrium Figure 3. The linearized tunneling current is $K_{tunnel}\delta x$ where δx is the deviation from the

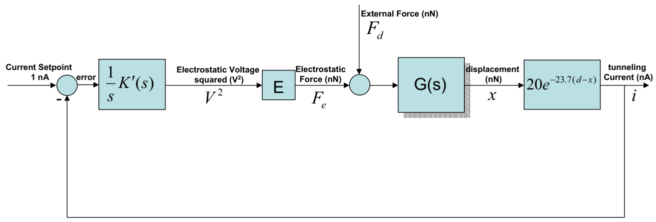

Fig. 2. Tunneling Accelerometer Feedback Loop

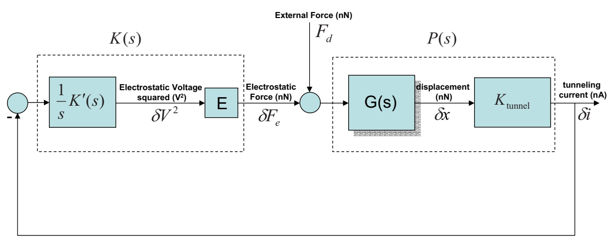

Fig. 3. Tunnelling Accelerometer Linearized Feedback Loop

operating distance corresponding to 1 nA of tunneling current. This distance is equal to 1 nm if the tunneling current is indeed given by $i = 20e^{-23.719(d-x)}$. The linearized gain at that operating point is $K_{tunnel} = 10^9 \times 20 \times 23.719 \times e^{-23.719} = 23.719$ nA/nm. While this value serves as a nominal value, K_{tunnel} there is considerable in its value. As pointed out earlier, the tunneling current parameters are typically unknown exactly and their values will gradually drift. For this reason, and because different devices will have different nominal values for all their parameters (not just tunneling parameters), a central objective of the design is to achieve stability and disturbance rejection that is robust to variations in K_{tunnel} away from the nominal value and to variations in the model parameters for $G(s)$.

We will use H_∞ loop-shaping design [11], [12] to meet the design objectives. By rejecting the effect of the disturbance F_d at the input of $G(s)$ robustly, we ensure that δF_e follows F_d over the frequencies where this rejection is achieved. In this case, the control signal V^2 necessary to achieve the rejection gives an accurate measure of the disturbance itself. This is the main principle of measurement of F_d. Clearly, the larger the frequency of the rejected disturbances, the larger the bandwidth of operation of the device. The limitation to the bandwidth ultimately comes from the measurement noise.

To meet the disturbance rejection requirements we shape the loop transfer function to be large over lower frequencies up to the control bandwidth. The plant is $P(s) = K_{tunnel}G(s)$. Figure 4 shows the plant frequency response and the desired loop shape $W(s)P(s)$ achieved by designing a pre-filter $W(s)$. The shaping filter is given by:

$$W(s) = 20\frac{(s+0.005)}{s(s+0.1)}.$$

Note that the weighting function includes an integrator. Since any stabilizing controller of $P(s)W(s)$ cannont cancel the pole at the origin, the final controller we get (which has $W(s)$ in its dynamics) will also include an integrator.

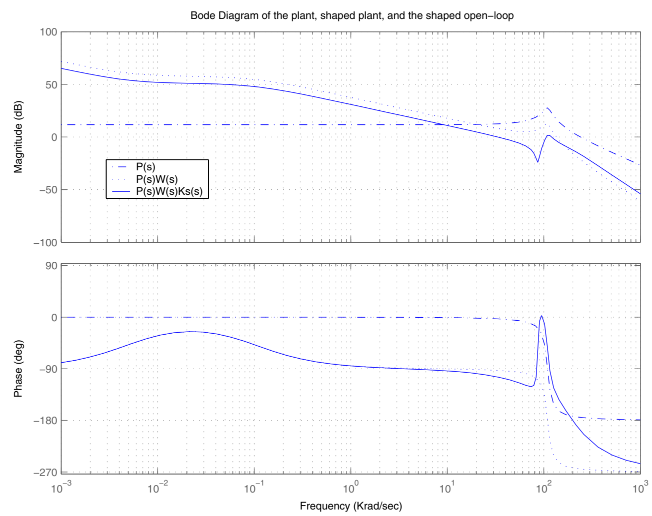

Fig. 4. Bode plot of the plant $P(s)$, the shaped plant $P(s)W(s)$, and $L(s) = P(s)W(s)K_s(s)$

The H_∞ loop-shaping technique was used to obtain a robustifying controller $K_s(s)$. The controller $K(s)$ is then given by $K(s) = W(s)K_s(s)$. For this design

$$K(s) = 43.2096\frac{(s+0.005016)(s^2+5.059s+7529)}{s(s+0.1)(s^2+235.5s+35260)}$$

and the controller $K'(s) = \frac{1}{E}sK(s)$. The designed loop gain $L(s) = G(s)W(s)K_s(s)$ is shown in Figure 4. For this design the gain margin is 12.322 dB and the phase margin is 71.3°. The bode plot of the plant $P(s)$ and $K(s)$ are shown in figure 5. The sensitivity function $S(s) = \frac{1}{1+P(s)K(s)}$ and the complementary sensitivity function $1-S(s)$ are plotted in figure 6. From the figure it is clear that disturbances between 0 and 10 Krad/s are well rejected.

IV. Nonlinear Simulations

Using the designed robust controller, simulations of the nonlinear system were performed. An external force signal F_d was generated and used to test the accelerometer. The external force and the response of the accelerometer variables to this force is shown in Figure 7.

It can be seen that the electrostatic force is the sum of two signals: a constant signal which is equal to the equilibrium value corresponding to a tunneling current reference step

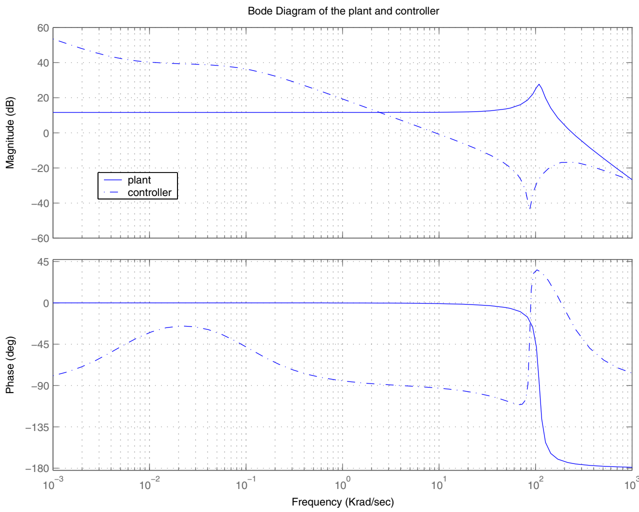

Fig. 5. Bode plot of the plant $P(s)$ and the controller $K(s)$

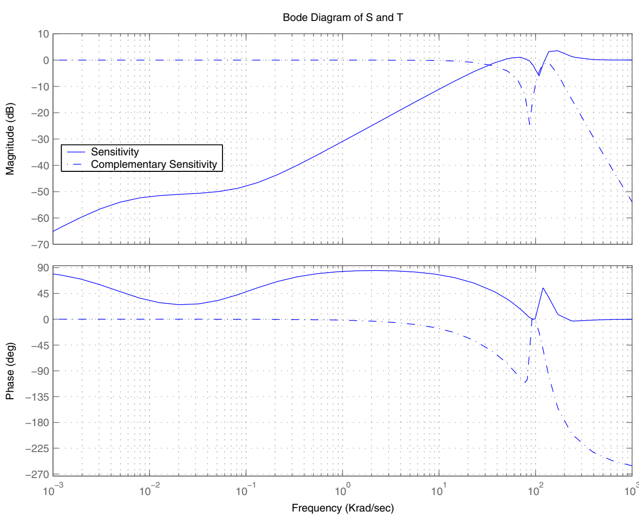

Fig. 6. Bode plot of the the sensitivity function and the complementary sensitivity function

with no external forces applied, and a second signal with is the response solely to the external force F_d. Since the purpose of this force is to reject the F_d its value follows $-F_d$. This force is related to the comb drive voltage-squared through mutliplication by E and therefore its value can easily be measured. As may be seen from the second plot, the nonconstant component of the electrostatic force gives a fairly accurate measure of the external force F_d. The sum of F_d and F_e is shown in Fig.7 (3rd plot). In the same figure, the fourth plot shows that the tunneling current is regulated to 1 nA. The fluctuations around this setpoint are due to the effect of F_d. The last plot in the figure shows the distance between the proof-mass and the tunneling tip.

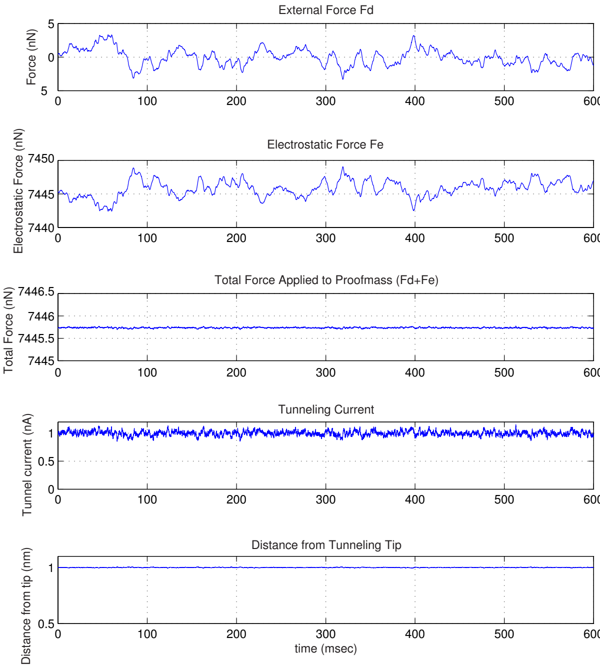

Fig. 7. The simulation plots shows (a) an external force F_d to be measured; (b) the electrostastic force in response to F_d; (c) the total forces acting on the proof-mass; (d) the tunneling current fluctuates around its nominal value of 1 nm; and (e) the distance from the proof-mass to the tunneling tip is effectively regulated to its nominal value of 1 nm

The distance is effectively maintained around 1nm with very little deviations.

To test the robustness of the system we first perturbed the bias V_b. The perturbed tunneling current relation becomes

$$i_p = 40e^{-23.719(d-x)}$$

which is 100% larger than the nominal value used in the design and first simulation. Next, the nominal proof-mass dynamics

$$G(s) = \frac{\frac{10^{-6}}{m}}{s^2 + 10^{-3}\frac{\omega_0}{Q}s + 10^{-6}{\omega_0}^2}.$$

were perturbed to $G_p(s)$ by decreasing $\frac{\omega_0}{Q}$ by 50% and increasing ${\omega_0}^2$ by 50%. Figure 8 shows the bode plot of $G(s)$ and $G_p(s)$. With both of these changes in place, and using the same robust controller as before, we repeated the nonlinear simulations. The results are shown in Figure 9.

This figure shows that the F_e signal continues to capture the F_d force very accurately despite the large change its equilibium value. Thus the performance of the device is virtually unaffected by the perturbations that were imposed. The tunneling current continues to be robustly regulated around its setpoint, while the distance of the proof-mass to the tunneling tip has slightly increased.

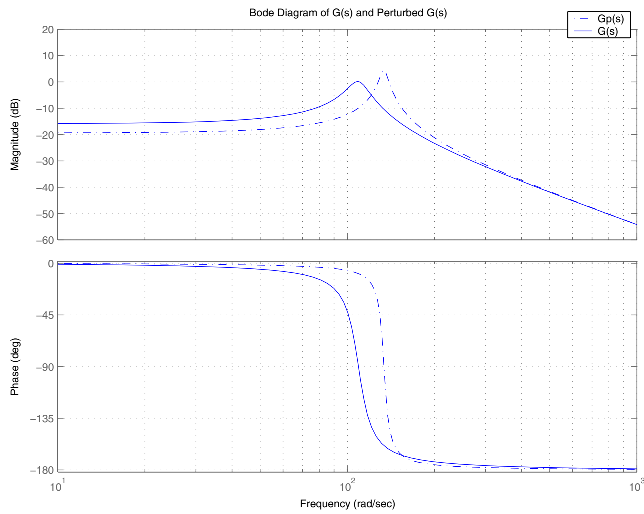

Fig. 8. Bode plot of the plant $P(s)$ and the controller $K(s)$

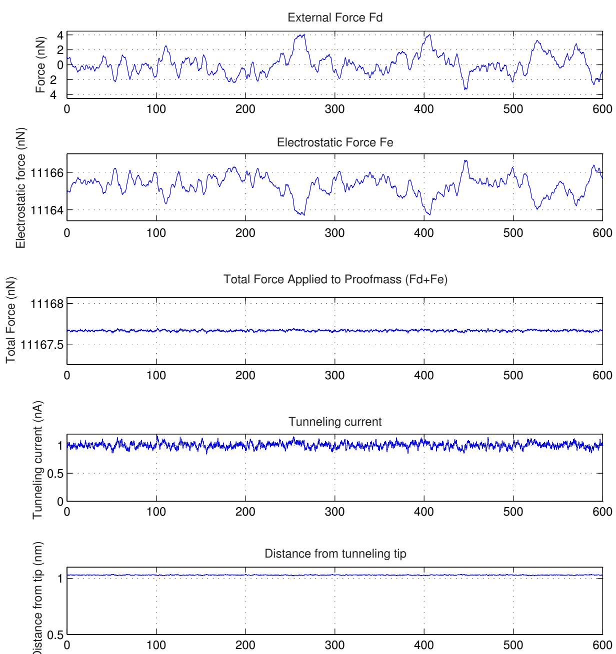

Fig. 9. Simulations of the nonlinear system after perturbing the device parameters while using the same robust controller. Note that the tunneling current is still regulated around its nominal value even though the regulated distance from the tunneling tip has increased

V. Conclusion

A robust controller has been designed for use in a tunneling accelerometer device. The design, which was achieved using H_∞ loop-shaping approach, resulted in a system that achieves high performance over its bandwidth and is robust to expected parameter variations. Experimental implementation of this controller onto a MEMS accelerometer is currently underway. Experimental results will be reported when they become available.

References

[1] Chang DT, Kubena RL, Stratton FP, Kirby DJ, Joyce RJ, Jinsoo Kim,"Wafer-bonded, high dynamic range, single-crystalline silicon tunneling accelerometer," *Proceedings of IEEE Sensors 2002, First IEEE International Conference on Sensors (Cat. No.02CH37394)* vol. 2, 2002, pp.860-3 vol.2, Piscataway, NJ, USA.

[2] Jing Wang, Yongjun Zhao, Tianhong Cui, Varahramyan K., "Synthesis of the modeling and control systems of a tunneling accelerometer using the MatLab simulation," *Journal of Micromechanics & Microengineering,* vol.12, no.6, Nov. 2002, pp.730-5. Publisher: IOP Publishing, UK.

[3] Cheng-Hsien Liu, Kenny TW, "A high-precision, Wide-bandwidth micromachined tunneling accelerometer," *Journal of Microelectromechanical Systems,* vol.10, no.3, Sept. 2001, pp.425-33. Publisher: IEEE, USA.

[4] Kubena RL, Stratton FP, Vickers-Kirby DJ, Joyce RJ, Chang DT, Schimert T, Gooch RW, "Low-cost tunneling accelerometer technology for high dynamic range applications," *Position Location and Navigation Symposium (Cat. No.00CH37062)* IEEE. 2000, pp.522-6. Piscataway, NJ, USA.

[5] Boyadzhyan V, Choma J Jr. "High temperature, high reliability integrated hybrid packaging for radiation hardened spacecraft micromachined tunneling accelerometer," *IEEE International Workshop on Integrated Power Packaging (Cat. No.98EX203)* 1998, pp.79-83. New York, NY, USA.

[6] Hartwell PG, Bertsch FM, Miller SA, Turner KL, MacDonald NC. "Single mask lateral tunneling accelerometer," *Proceedings of Eleventh Annual International Workshop on Micro Electro Mechanical Systems. An Investigation of Micro Structures, Sensors, Actuators, Machines and Systems (Cat. No.98CH36176),* 1998, pp.340-4. New York, NY, USA.

[7] Cheng-Hsien Liu, Barzilai AM, Reynolds JK, Partridge A, Kenny TW, Grade JD, Rockstad HK, "Characterization of a high-sensitivity micromachined tunneling accelerometer with micro-g resolution," *Journal of Microelectromechanical Systems,* vol.7, no.2, June 1998, pp.235-44. Publisher: IEEE, USA.

[8] Scheeper PR, Reynolds JK, Kenny TW. Development of a modal analysis accelerometer based on a tunneling displacement transducer," *Tranducers 97, 1997 International Conference on Solid-State Sensors and Actuators. Digest of Technical Papers (Cat. No.97TH8267),* Part vol.2, 1997, pp.867-70 vol.2. New York, NY, USA.

[9] Rockstad HK, Kenny TW, Kelly PJ, Gabrielson TB, "A microfabricated electron-tunneling accelerometer as a directional underwater acoustic sensor," *American Institute of Physics Conference Proceedings,* no.368, 1996, pp.57-68. USA.

[10] T. B. Gabrielson, "Mechanical-thermal noise in micromachined acoustic and vibration sensors," *IEEE transactions on Electron Devices,* vol. 40, p. 903, 1993.

[11] McFarlane, D.C.and K. Glover, "Robust controller design using normalised coprime factor plant descriptions," *Springer Verlag, Lecture Notes in Control and Information Sciences,* vol. 138, 1989.

[12] McFarlane, D.C., and K. Glover, "A loop shaping design procedure using synthesis," *IEEE Transactions on Automatic Control,* vol. 37, no. 6, pp. 759-769, June 1992.